Hindawi Publishing Corporation
Mathematical Problems in Engineering
Volume 2015, Article ID 936493, 7 pages
http://dx.doi.org/10.1155/2015/936493

Research Article

Design and Analysis of a Novel 25 GHz Interleaver for DWDM Applications with Two Ring Configurations

Tsair-Chun Liang and Chun-Ting Chen

Graduate Institute of Electrical Engineering, National Kaohsiung First University of Science and Technology, Kaohsiung City 811, Taiwan

Correspondence should be addressed to Tsair-Chun Liang; tcliang@nkfust.edu.tw

Received 19 June 2014; Accepted 2 August 2014

Academic Editor: Teen-Hang Meen

We present a novel scheme of an excellent flat-top 25 GHz optical interleaver based on two ring configurations. And the Advanced Systems Analysis Program (ASAP) optical modeling software has been utilized for the interleaver design. The optical path difference for interference and the phase shift are provided by the interferometer with two birefringent crystals and dual-ring arrangement. The proposed structure exhibits the passband utilization of more than 90% and the channel isolation greater than 95 dB within the C-band. Furthermore, we improve the dispersion performance by employing $\lambda/6$ wave plates as birefringent compensators for interleavers. The research results illustrate that our proposed scheme with compensator can improve the dispersion of more than 85.8%. Comparing the performance with the previous studies of optical interleavers with birefringent crystal and ring structure, the proposed system can achieve an excellent 25 GHz multichannel filter for dense wavelength division multiplexing (DWDM) transmission systems.

1. Introduction

Due to the growing demand for network communications capacity, dense wavelength division multiplexing (DWDM) [1, 2] has emerged as vital component for optical fiber networks. Several techniques for flexibility in all-optics dynamic networks have been engaged in DWDM systems [3, 4]. And how to increase the number of channels is an important issue [5]. A spectral interleaver is capable of separating a set of channels into two sets twice the channel spacing. An optical interleaver has been verified as an effective technique in increasing channel counts by doubling or quadrupling the number of optical channels when the channel spacing is in the range of 0.2 nm [6–8].

Conventional interleavers are based on interferometers that employ Gires-Tournois etalons (GTEs) as a phase-dispersion element [9, 10]. These interferometers employ a polarization beam splitter (PBS) to split the input signal into two beams and then recombine them at the beam splitter by using two GTEs to provide the redirection path; these interferometers can be Michelson interferometers or Mach-Zehnder interferometers. When a path length difference exists between the two interfering beams, these conventional interleavers provide a square-like spectrum transmission function. However, in conventional etalons involving thin film coatings, the performance is often optimized in a small spectral region within the C-band. They cannot carry on the entire C-band.

To provide a uniform performance over the entire C-band, the partial reflecting mirrors of the optical resonator must maintain constant reflectivity over the entire C-band. Such requirements are difficult to achieve by using conventional thin-film coating technology. In this research, the Advanced Systems Analysis Program (ASAP) [11] optical modeling software has been utilized for the interleaver design. The ASAP model is configured based on the actual component parameters that compared with the actual size is 1 : 1. The greatest shortcoming of conventional interleavers is an inferior dispersion. In this study, we propose a new scheme of birefringent optical interleaver employing dual-ring structures including the quarter-wave ($\lambda/4$) plates, trapezoid prisms, and the $\lambda/6$ wave plates to improve the dispersion.

The next section presents the design procedures of a high performance interleaver using quarter-wave ($\lambda/4$) plates and

polarization optics. Then the design of an improved structure of interleaver is illustrated. We can get a very good dispersion improvement to employ this proposed configuration. The simulation result is performed to evaluate the performance of this design method in Section 3. Finally, we conclude this paper in Section 4.

2. The Proposed Interleaver Based on Two Ring Configurations

Figure 1 shows the schematic configuration (noncompensation) of the dual-ring structure based birefringent optical interleaver consisting of two birefringent crystals (the length of YVO_4 is 30 mm), two trapezoid prisms (transmission rate is 91.4% and refraction index is 1.6), a polarization beam splitter (PBS), two $\lambda/4$ wave plates, and four highly reflective mirrors (reflectivity is 99.8%). A beam of unpolarized light is transmitting through the PBS, and then the beams are directed toward the YVO_4 birefringent crystal and the quarter-wave plate ($\lambda/4$ @ 45°). The YVO_4 birefringent crystal is used for appropriate retardance of interference. The quarter-wave plate is employed to rotate the polarization states of these two beams by 45 degrees. As a result, the beams inside the birefringent crystals consist of both ordinary and extraordinary waves, but with equal amplitudes. While the beams propagate inside the birefringent crystals, a phase retardation exists between these two waves at the end of the crystals. These beams, consisting of both ordinary and extraordinary waves, are then directed toward the ring structure, as shown in Figure 1.

In both birefringent crystals (see Figure 1), the ordinary wave corresponds to the s-wave while the extraordinary one corresponds to the p-wave. The trapezoid prism interface of the ring structure exhibits different Fresnel reflectivities for these two polarization components (s- and p-) of the beam. As a result of these different reflectivities, the two polarization components experience further phase retardation by the quarter-wave plate ($\lambda/4$ @ 45°) after the birefringent crystal and different phase shifts upon transmitting (or reflecting) through the ring arrangement. Before both components of the beam are mixed and recombined by the PBS, a phase retardation by the birefringent crystal reoccurs again. The birefringent crystal (YVO_4) acts as an interferometer, and the ring structure is configured by a prism and two mirrors (with air in the resonator). The ring configuration, acting as a Gires-Tounois Etalon, is formed by the mirrors M_1, M_2 and M_3, M_4 and the prism-air interface which are aligned perpendicularwise to the light beams.

The prism is cut in a trapezoid-shape to provide the appropriate angle of incidence so that the desired Fresnel reflectivities, R_o and R_e, are obtained and R_e and R_o are the reflectivity of the air-prism interface for the e-component (extraordinary beam) and o-component (ordinary beam). The normalized intensity of one of the output ports can be expressed as follows [13–15]:

$$I_1 = \frac{I_0}{2}\left[1 + \cos\left(\frac{4\pi}{\lambda}\Delta nL + (\phi_e - \phi_0)\right)\right], \tag{1}$$

where I_0 is the intensity of the unpolarized incident beam and L is the length of the two birefringent crystals, ϕ_e and ϕ_o are the phase shifts of the beam upon reflection from the ring structure, and ($\Delta n = n_e - n_o$) is the refractive index difference of n_e and n_o. The channel isolation of the interleaver with the dual-ring structure is near 95 dB, and the calculated results of the stopband and channel isolation of a 25 GHz channel spacing application, odd channels and even channels of partial C-band, are shown in Figures 2(a) and 2(b), respectively. In Figure 2, the 25 dB stopband was found to be 0.173 nm (21.625 GHz) and a 0.5 dB wide passband of 0.156 nm (19.5 GHz); hence, we can reach the passband utilization of 90.17% (=0.156 nm/0.173 nm × 100%). And the channel isolation of the interleaver is greater than 95 dB. The higher passband utilization means that the output was closer to square wave results. The more close to a square wave output, the better the performance of interleaver. These results clearly indicate that an interleaver with a ring structure can provide a wide 0.5 dB passband and a good 25 dB stopband.

3. Optimal Design of Improved Dispersion Interleaver by Compensators

Chromatic dispersion compensation is the most deserving progress in this study. This interleaver with improved dispersion compensation is shown in Figure 3. The polarization azimuth angle of the birefringent crystal [16–19] is obtained by employing $\lambda/4$ wave plates ($\lambda/4$ @ 45°) and $\lambda/6$ wave plates ($\lambda/6$ @ 30°). The phase shifts of $\lambda/4$ wave plates and $\lambda/6$ wave plates can be expressed as (2) and (3), respectively:

$$\begin{aligned}|w_1| &= |R(-\psi)\, w_0 R(\psi)| \\ &= \left|\frac{1}{\sqrt{2}}\begin{pmatrix}1 & -1\\ 1 & 1\end{pmatrix}\begin{pmatrix}e^{-i\pi/4} & 0\\ 0 & e^{i\pi/4}\end{pmatrix}\frac{1}{\sqrt{2}}\begin{pmatrix}1 & 1\\ -1 & 1\end{pmatrix}\right| \\ &= 1.414,\end{aligned} \tag{2}$$

$$\begin{aligned}|w_2| &= |R(-\psi)\, w_0 R(\psi)| \\ &= \left|\frac{1}{2}\begin{pmatrix}\sqrt{3} & -1\\ 1 & \sqrt{3}\end{pmatrix}\begin{pmatrix}e^{-i\pi/6} & 0\\ 0 & e^{i\pi/6}\end{pmatrix}\frac{1}{2}\begin{pmatrix}\sqrt{3} & 1\\ -1 & \sqrt{3}\end{pmatrix}\right| = 1.75,\end{aligned} \tag{3}$$

where w_1 and w_2 are the round-trip phase shift inside the ring structure of $\lambda/4$ wave plates and $\lambda/6$ wave plates, respectively. $R(\psi)$ is the coordinate rotation matrix and w_0 is the Jones matrix depending on the retarder plates.

The output group delay after compensation can be viewed as the average group delay from two modes, $\tau(\omega) = [\tau_e(\omega) + \tau_0(\omega)]/2$, where $\omega = 2\pi c/\lambda$ is the optical angular frequency and can be demonstrated as

$$\tau(\omega) = \frac{T}{2}\left\{\frac{(1 - R_0)}{1 + R_0 - 2\sqrt{R_0}\cos\left[(4\pi/\lambda)\, L_R\right]} + \left(1 - \left[\frac{R_e}{(w_1^2 + w_2^3)}\right]\right)\right.$$

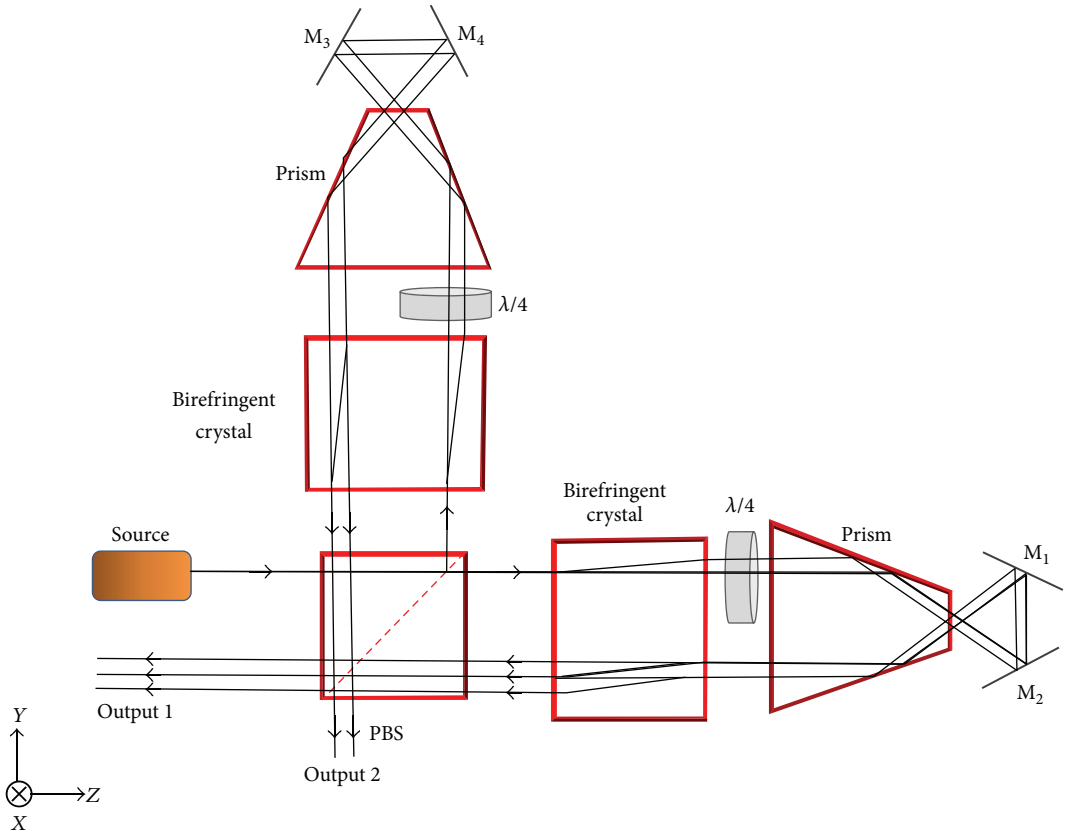

FIGURE 1: A schematic drawing of a 25 GHz channel spacing interleaver based on two ring configurations.

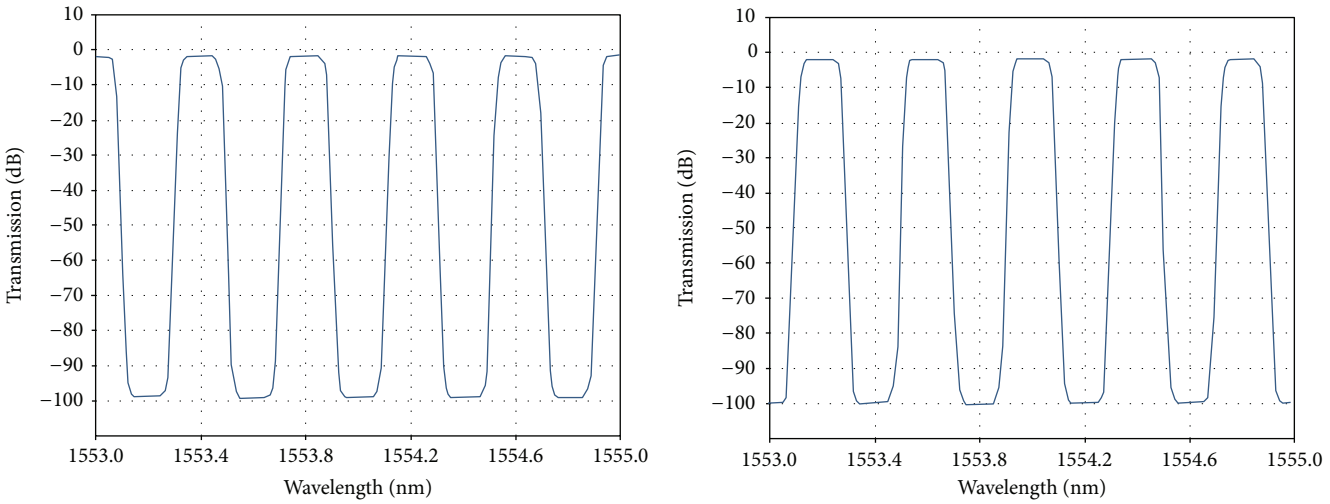

FIGURE 2: The transmission of a 25 GHz interleaver, passband utilization of 95.49%: (a) output port 1 (partial odd channels) and (b) output port 2 (partial even channels) of C-band.

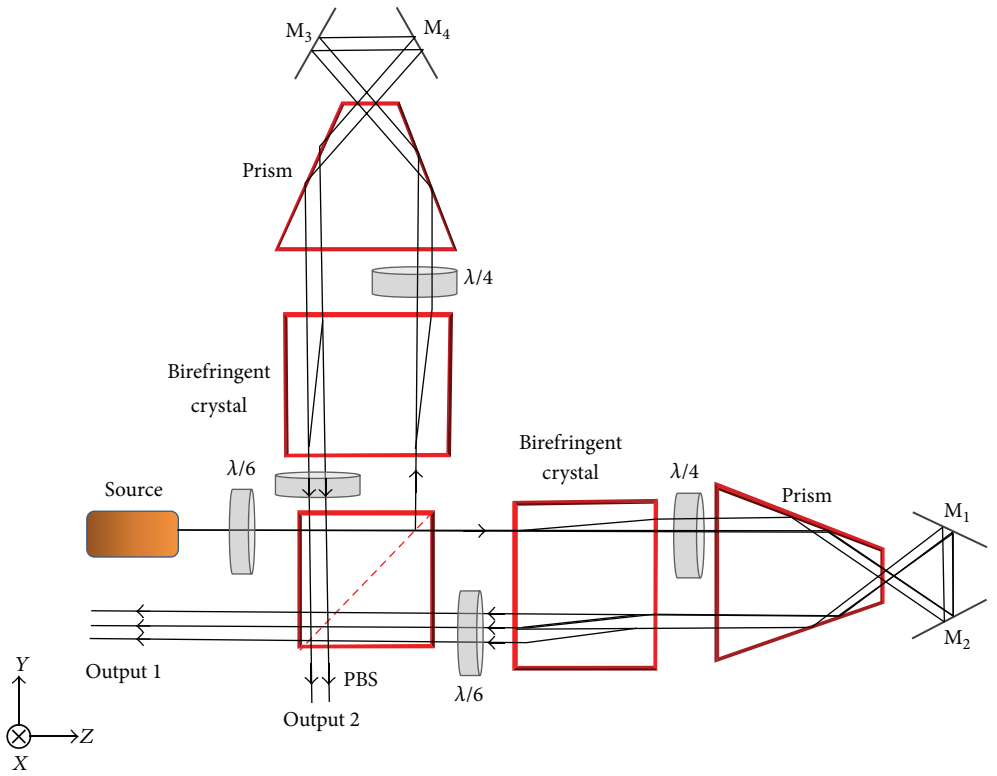

Figure 3: The ASAP layout of improved dispersion configuration.

$$\times\left(1+\left[\frac{R_e}{(w_1^2+w_2^3)}\right]\right.$$
$$\left.-2\left[\frac{R_e}{(w_1^2+w_2^3)}\right]^{1/2}\cos\left[\left(\frac{4\pi}{\lambda}\right)L_R\right]\right)^{-1}\Bigg\}. \quad (4)$$

In (4), L_R is the round-trip optical path of the ring structure, $T = L_R/c$ is the round-trip time, and $\lambda = c/\nu$. Both w_1 and w_2 are the transmission matrixes of $\lambda/4$ wave plates and $\lambda/6$ wave plates, respectively. After the dispersion is compensated, the configuration as shown in Figure 3, the group velocity dispersion (GVD) is given by $D(\lambda) = d\tau/d\lambda$ [ps/nm] and can be expressed as follows:

$$D(\lambda) = \frac{4\pi L_R T \sin\left((4\pi/\lambda)L_R\right)}{\lambda^2}$$
$$\times\left\{\frac{(R_0)^{1/2}(1-R_0)}{\left[1+R_0-2(R_0)^{1/2}\cos\left((4\pi/\lambda)L_R\right)\right]^2}\right.$$
$$\left.+\left(\left[\frac{(R_e)}{(w_1^2+w_2^3)}\right]^{1/2}\left[1-\left(\frac{R_e}{(w_1^2+w_2^3)}\right)\right]\right)\right.$$
$$\times\left(\left[1+\left(\frac{R_e}{(w_1^2+w_2^3)}\right)-2\left(\frac{R_e}{(w_1^2+w_2^3)}\right)^{1/2}\right.\right.$$
$$\left.\left.\times\cos\left(\left(\frac{4\pi}{\lambda}\right)L_R\right)\right]^2\right)^{-1}\Bigg\}. \quad (5)$$

Figure 4 shows the path of the ring cavity which is configured by a trapezoid prism and two mirrors. The incident light hits trapezoid prism at a perpendicular angle and total reflects by the second surface, and finally transmits through the first surface of prism perpendicular again. In Figure 4, θ_1 and θ_2 are the incident and transmitted angles at third surface, and n_1 and n_2 are the reflective indices of prism and air, respectively. At the prism-air surface, the different Fresnel reflectivities for ordinary wave and extraordinary wave (s- and p-polarization components) can be presented by [6]

$$R_0 = \left|\frac{n_1\cos\theta_1 - n_2\cos\theta_2}{n_1\cos\theta_1 + n_2\cos\theta_2}\right|^2,$$
$$R_e = \left|\frac{n_2\cos\theta_1 - n_1\cos\theta_2}{n_2\cos\theta_1 + n_1\cos\theta_2}\right|^2. \quad (6)$$

According to (1) and (5), calculated by the simulation software ASAP, we can get normalized intensity of the output

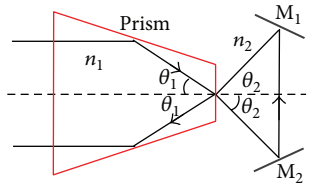

FIGURE 4: Optical path between the prism and air schematic chart.

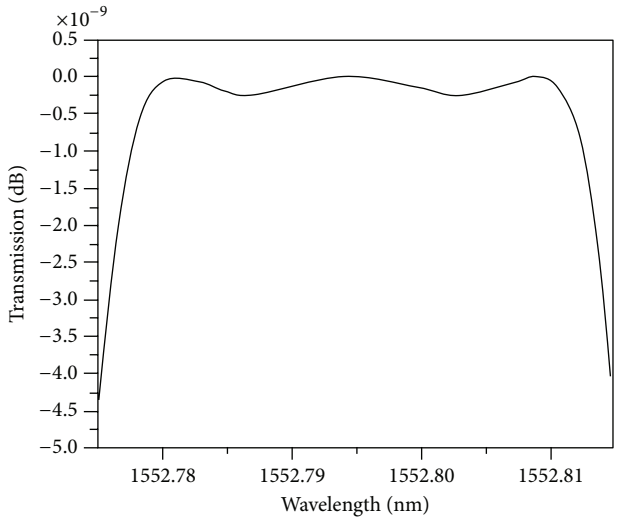

FIGURE 5: The simulation result of the flat-top ripple in a 25 GHz channel spacing.

channels and their chromatic dispersion. In this study, the optimum incident angle θ_1 is about 34.5°. At this angle of incidence, the reflectivities of the flat-top bandwidth interleaver are about R_o = 17.01% and R_e = 8.39%. And the ripple of output power intensity of the 25 GHz channel spacing is 0.227397×10^{-9} dB (see Figure 5). Figure 6 shows that the dispersion comparison of a 25 GHz channel spacing of partial C-band with- and without-compensation. The research results illustrate that our modified scheme can improve the dispersion of more than 85.8% (=(1524.3–215.93)/1524.3). The effect of improved dispersion of a 25 GHz interleaver can be observed, as shown in Figure 7. The optical intensities of without-compensating and with-compensating schemes are 0.546 a.u. and 0.936 a.u., respectively. The eye diagrams for 10 Gb/s application of with-compensation and without-compensation by pseudorandom binary sequence (PRBS) (2^{31}-1) have been measured, as shown in Figure 8. The research results are compared with other related issues such as a ring-cavity architecture system [6, 12] and using Gires-Tournois etalons as phase dispersive mirrors in a Michelson interferometer system [9] (see Table 1).

4. Conclusions

We have analyzed a flat-top 25 GHz optical interleaver based on a dual-ring architecture with fewer components. Compared to previous studies, our interleaver exhibited a 0.5 dB

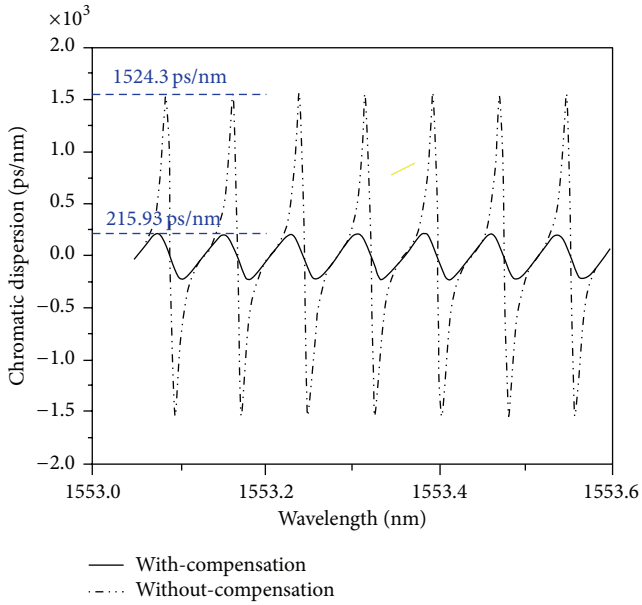

FIGURE 6: The chromatic dispersion comparison between with-compensation and without-compensation of a 25 GHz channel spacing of partial C-band.

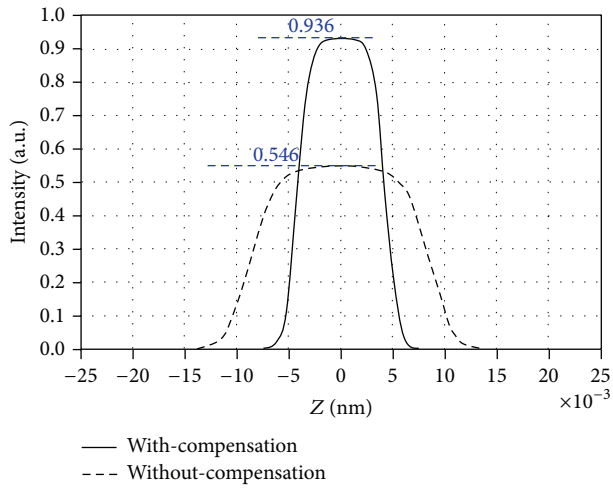

FIGURE 7: The optical intensity comparisons of a 25 GHz channel spacing: the calculated intensities are 0.936 a.u. of with-compensation and 0.546 a.u. of without-compensation.

passband larger than 0.156 nm (19.5 GHz), a 25 dB stopband greater than 0.173 nm (21.625 GHz), a channel isolation greater than 95 dB, and an excellent flat-top ripple, which is smaller than 0.227×10^{-9} dB. The benefit of this interleaver is that it utilizes the Fresnel principle to achieve precise reflectivity. Unlike dielectric mirrors with thin-film coatings, the reflectivities of the Fresnel reflection are insensitive to wavelength variations in the transmission band. Uniform reflectivities are essential to ensure the same performance over the entire C-band. In particular, the novel interleaver can simultaneously produce an excellent performance of chromatic dispersion which can achieve an improvement of

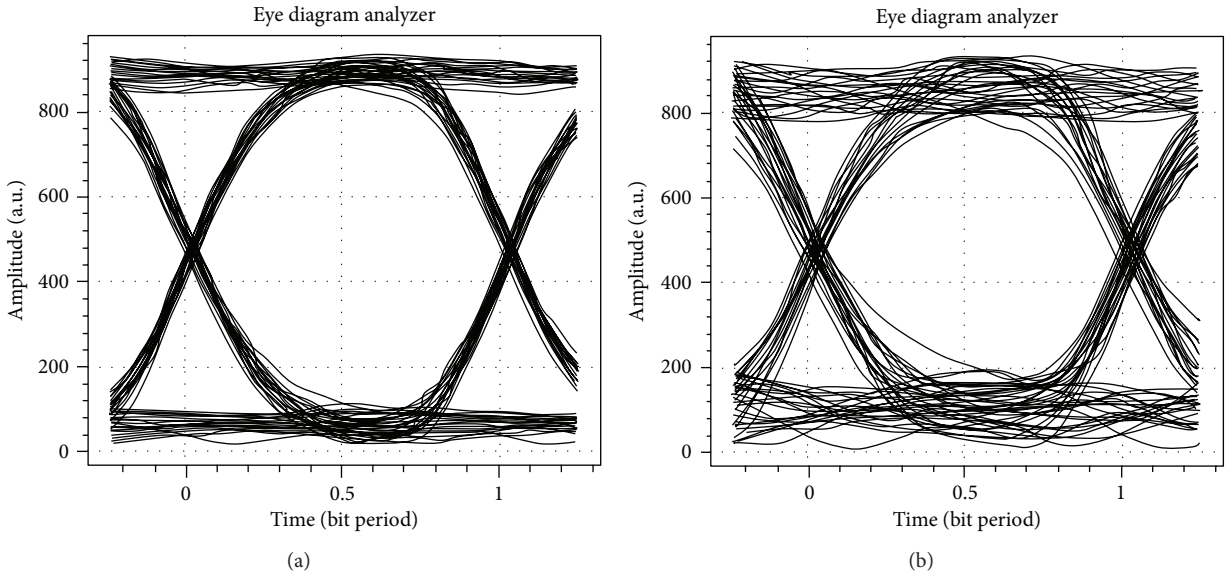

Figure 8: The eye diagrams by PRBS 2^{31}-1 for 10 Gb/s application (a) with-compensation and (b) without-compensation.

Table 1: The characteristics comparison of interleaver systems.

Characteristics	System type			
	Lee et al. [6]	Lee et al. [12]	Hsieh et al. [9]	This work
Filter channel spacing	25 GHz	25 GHz	50 GHz	25 GHz
Structure technique	Sagnac interferometer and ring cavity	Ring cavity	Gires-Tournois etalons	Two-ring cavity
Channel isolation (dB)	45	>36	30	95
0.5 dB passband (nm)	0.182	>0.145	0.35	0.156
25 dB stopband (nm)	0.155	>0.145	0.32	0.173
Flat-top ripple (dB)	$<10^{-3}$	$\sim 10^{-3}$	NA	0.227×10^{-9}

85.8% when we modify the interleavers structure by $\lambda/6$ wave plates. This unique interleaver is suitable for capacity upgrade in DWDM and FTTx applications.

Conflict of Interests

The authors declare that there is no conflict of interests regarding the publication of this paper.

Acknowledgment

The authors would like to gratefully acknowledge the Ministry of Science and Technology of Taiwan for their funding support under MOST 103-2622-E-327-007-CC3.

References

[1] T. Liang and S. Hsu, "The L-band EDFA of high clamped gain and low noise figure implemented using fiber Bragg grating and double-pass method," *Optics Communications*, vol. 281, no. 5, pp. 1134–1139, 2008.

[2] S. V. Kartalopoulos, *Introduction to DWDM Technology: Data in a Rainbow*, chapter 1, IEEE Press, New York, NY, USA, 2000.

[3] T. C. Liang, C. M. Tsai, and B. C. Wu, "A wavelength routing device by using cyclic AWGs and tunable FBGs," *Optical Fiber Technology*, vol. 19, no. 3, pp. 189–193, 2013.

[4] R. Saunders, "Coherent DWDM technology for high speed optical communications," *Optical Fiber Technology*, vol. 17, no. 5, pp. 445–451, 2011.

[5] R. Casellas, R. Muñoz, J. M. Fàbrega et al., "GMPLS/PCE control of flexi-grid DWDM optical networks using CO-OFDM transmission," *Journal of Optical Communications and Networking*, vol. 4, no. 11, Article ID 6360163, pp. B1–B10, 2012.

[6] C. W. Lee, R. Wang, P. Yeh, and W. H. Cheng, "A flat-top birefringent interleaver based on ring-cavity architecture," *Optics Communications*, vol. 260, no. 1, pp. 311–317, 2006.

[7] A. Zeng, X.-G. Ye, J. Chon, and F. Liang, "25 GHz interleavers with ultra-low chromatic dispersion," in *Proceedings of the Optical Fiber Communication Conference and Exhibit (OFC '02)*, pp. 396–398, March 2002.

[8] T. C. Liang and C. T. Chen, "Investigation of dispersion and performance based on ring cavity by birefringent interleaver for DWDM transmission systems," *Mathematical Problems in Engineering*, vol. 2013, Article ID 740412, 5 pages, 2013.

[9] C. Hsieh, R. Wang, Z. J. Wen et al., "Flat-top interleavers using two Gires-Tournois etalons as phase-dispersive mirrors in a Michelson interferometer," *IEEE Photonics Technology Letters*, vol. 15, no. 2, pp. 242–244, 2003.

[10] J. Zhang and X. Yang, "Universal Michelson Gires-Tournois interferometer optical interleaver based on digital signal processing," *Optics Express*, vol. 18, no. 5, pp. 5075–5088, 2010.

[11] ASAP (Advanced Systems Analysis Program), Breault Research Organization Inc, Tucson, Ariz, USA.

[12] C. Lee, R. Wang, P. Yeh, and W. Cheng, "Sagnac interferometer based flat-top birefringent interleaver," *Optics Express*, vol. 14, no. 11, pp. 4636–4643, 2006.

[13] P. Yeh, *Optical Waves in Layered Media*, John Wiley & Sons, New York, NY, USA, 1998.

[14] S. Cao, J. Chen, J. N. Damask et al., "Interleaver technology: comparisons and applications requirements," *Journal of Lightwave Technology*, vol. 22, no. 1, pp. 281–289, 2004.

[15] B. B. Dingel and M. Izutsu, "Multifunction optical filter with a Michelson-Gires-Tournois interferometer for wavelength-division-multiplexed network system applications," *Optics Letters*, vol. 23, no. 14, pp. 1099–1101, 1998.

[16] L. Wei and J. W. Y. Lit, "Design optimization of flattop interleaver and its dispersion compensation," *Optics Express*, vol. 15, no. 10, pp. 6439–6457, 2007.

[17] J. Zhang, L. Lin, and Y. Zhou, "Novel and simple approach for designing lattice-form interleaver filter," *Optics Express*, vol. 11, no. 18, pp. 2217–2224, 2003.

[18] M. Oguma, T. Kitoh, Y. Inoue et al., "Compact and low-loss interleave filter employing lattice-form structure and silica-based waveguide," *Journal of Lightwave Technology*, vol. 22, no. 3, pp. 895–902, 2004.

[19] K. Jinguji and M. Oguma, "Optical half-band filters," *Journal of Lightwave Technology*, vol. 18, no. 2, pp. 252–259, 2000.